Immune Network
http://dx.doi.org/10.4110/in.2014.14.1.54
pISSN 1598-2629 eISSN 2092-6685
ORIGINAL ARTICLE

Molecular Characterization of Neurally Differentiated Human Bone Marrow-derived Clonal Mesenchymal Stem Cells

TacGhee Yi[1,2,4#], *Hyun-Joo Lee*[3#], *Yun-Kyoung Cho*[4], *Myung-Shin Jeon*[1,2]* *and Sun U. Song*[1,4]*

[1]Translational Research Center, [2]Inha Research Institute for Medical Sciences of Biomedical Sciences, and [3]Drug Development Program, Department of Medicine, Inha University School of Medicine, Incheon 400-712, [4]HomeoTherapy Co. Ltd., Incheon 400-711, Korea

Bone marrow-derived mesenchymal stem cells (MSCs) are multipotent, with the ability to differentiate into different cell types. Additionally, the immunomodulatory activity of MSCs can downregulate inflammatory responses. The use of MSCs to repair injured tissues and treat inflammation, including in neuroimmune diseases, has been extensively explored. Although MSCs have emerged as a promising resource for the treatment of neuroimmune diseases, attempts to define the molecular properties of MSCs have been limited by the heterogeneity of MSC populations. We recently developed a new method, the subfractionation culturing method, to isolate homogeneous human clonal MSCs (hcMSCs). The hcMSCs were able to differentiate into fat, cartilage, bone, neuroglia, and liver cell types. In this study, to better understand the properties of neurally differentiated MSCs, gene expression in highly homogeneous hcMSCs was analyzed. Neural differentiation of hcMSCs was induced for 14 days. Thereafter, RNA and genomic DNA was isolated and subjected to microarray analysis and DNA methylation array analysis, respectively. We correlated the transcriptome of hcMSCs during neural differentiation with the DNA methylation status. Here, we describe and discuss the gene expression profile of neurally differentiated hcMSCs. These findings will expand our understanding of the molecular properties of MSCs and contribute to the development of cell therapy for neuroimmune diseases.
[Immune Network 2014;14(1):54-65]

INTRODUCTION

Adult stem cells have lineage-restricted differentiation potential. They are generally named according to their tissue of origin, for example, as mesenchymal stem cells (MSCs), hematopoietic stem cells, and endothelial progenitor cells. MSCs have been isolated from various mesenchymal tissues, including bone marrow (BM), adipose tissue, and umbilical cord blood (1,2). Because of their multifaceted immunomodulatory functions, MSCs have emerged as an attractive therapeutic approach for the treatment of immune diseases (3). A number of studies have shown that MSCs are effective in treating immune-related or inflammatory diseases such as graft-versus-host disease, colitis, and pancreatitis (4-6).

Multilineage plasticity is another property of MSCs. MSCs can differentiate into various cell types found in mesenchymal tissues, such as osteocytes, chondrocytes, and adipocytes (7). MSCs can differentiate into ectodermal, endodermal, and mesodermal lineages (8,9). MSCs have been used to repair spinal

Received on December 10, 2013. Revised on February 4, 2014. Accepted on February 4, 2014.

*Corresponding Authors. Sun U. Song, Translational Research Center, Inha University School of Medicine, 7-206 Shinheung 3-ga, Jung-gu, Incheon, Korea. Tel: 82-32-890-2460; Fax: 82-32-890-2460; E-mail: sunuksong@inha.ac.kr, Myung-Shin Jeon, Translational Research Center, Inha University School of Medicine, 7-206 Shinheung 3-ga, Jung-gu, Incheon, Korea. Tel: 82-32-890-3682; Fax: 82-32-890-2460; E-mail: msjeon@inha.ac.kr
#These authors equally contributed to this work.

Keywords: hcMSC, Mesenchymal stem cell, Neural differentiation, Microarray, Methylation, Subfractionation culturing method

Abbreviations: MSC, mesenchymal stem cell; hcMSC, human clonal mesenchymal stem cell; SCM, subfractionation culturing method; BM, bone marrow

cord injury *in vivo* and to promote neuronal recovery (10). In addition, MSCs can adopt neuronal and glial phenotypes *in vitro* under the appropriate conditions (11,12). Whether the neuronal morphology observed during the neurogenic differentiation of MSCs is an artifact induced by the neurogenic medium is controversial (13,14), but several studies have presented evidence supporting the neural differentiation potential of MSCs (15,16).

Furthermore, MSCs are considered a potent therapeutic tool likely to have practical use in the near future. There have been extensive efforts over the past decade to treat various incurable diseases using stem cells, including neuroimmune disorders such as spinal cord injury, stroke, and multiple sclerosis (17). Because they are multipotent and immunomodulatory, neural stem cells or neural precursor cells are a therapeutic option for the treatment of neuroimmune diseases (18,19). However, considering the simplicity of stem cell isolation, the ease of cell expansion, and the wide range of applicability, MSCs offer a good alternative for the treatment of neuroimmune diseases, particularly given their neuroglial potential and immunomodulatory properties. Therefore, a detailed characterization of neurally differentiated MSCs is needed to improve cell-based treatments for neuroimmune diseases.

The density-gradient centrifugation method is the most popular technique for isolating MSCs from BM (20). MSCs obtained by this method are heterogeneous because they contain mixed populations of MSCs. Although all of the cells possess MSC characteristics, their cell surface marker expression, differentiation potential, and cytokine secretion vary, suggesting that BM contains a variety of MSC populations with different biological capacities (21). Studies of heterogeneous MSCs have been informative, but the heterogeneity of the cell population likely affects the interpretation of data acquired from experiments with these cells. In light of this shortcoming, we recently developed a novel method, the subfractionation culturing method (SCM), to isolate and establish homogeneous human clonal MSCs (hcMSCs) from small aspirates of human BM (21). hcMSC lines established with our protocol express well-known MSC markers and differentiate into various cell types, including osteocytes, chondrocytes, and adipocytes. Additionally, the hcMSC clones express neural or hepatocytic phenotypes after neural or hepatogenic differentiation *in vitro*.

Although several microarray analyses have examined the expression profiles of MSCs (22,23), we could not find any studies that analyzed gene expression in homogeneous clonal MSCs during differentiation. Because a number of MSC populations with different differentiation potentials might be present in the BM (21), we used hcMSCs with high neurogliogenic potency to compare gene expression before and after neural differentiation. In this study, we verified the neural potency of highly homogeneous hcMSCs and used microarray analysis to assess gene expression during their differentiation into neuroglial cells. Additionally, we performed CpG methylation array analysis and compared methylation status with gene expression to obtain a more reliable profile of gene expression in neurally differentiated hcMSCs.

MATERIALS AND METHODS

Isolation of hcMSCs and cell surface phenotyping using flow cytometry

BM aspirates were taken from the iliac crest of a healthy male donor after informed consent was provided (approved by the INHA University Medical School Institutional Review Board; IRB Number 10-51). Isolation of hcMSCs was carried out as previously described (21). Several cell surface antigens on the established hcMSC line, named KBHD502, were characterized by flow cytometry. The antibodies used for the analysis were anti-CD14, anti-CD29, anti-CD31, anti-CD34, anti-CD44, anti-CD73, anti-CD90, anti-CD105, anti-CD119, anti-CD133, anti-CD166, anti-HLA class I, anti-HLA-DR, anti-Stro-1, anti-c-Met, and anti-c-Kit (BD Biosciences Pharmingen, San Diego, CA, USA). The cells were analyzed in a FACSCalibur flow cytometer (BD Biosciences). Isotype-matched control antibodies were used as controls.

In vitro immunosuppression assay

The *in vitro* immunosuppressive activity of hcMSCs was determined by [^{3}H]-thymidine incorporation. Briefly, 2×10^5 peripheral blood mononuclear cells (PBMCs) from two different healthy donors (1×10^5 cells each) were mixed and cultured in a 96-well plate for mixed lymphocyte reactions. hcMSCs (4×10^4 cells) were co-cultured at a ratio of 1:5 (hcMSCs: PBMCs) in these reactions. [^{3}H]-thymidine (1 μCi/reaction) was added for the last 12～16 h of culture. Radioactivity was measured in a beta-counter.

In vitro neural differentiation and immunofluorescence (IF) staining

For IF staining, the cells were seeded onto an 8-well chamber

slide (Nunc, Naperville, IL, USA) at a density of 1×10^4 cells/well. After a 24-h incubation, the growth medium was removed and replaced with neurogenic differentiation medium (neurobasal medium supplemented with B27 supplement (Gibco-BRL, Gaithersburg, MD, USA), 1 mM dibutyryl cAMP (Sigma-Aldrich, St. Louis, MO, USA), 0.5 mM 1-methyl-3-isobutylxanthine (Sigma-Aldrich), 20 ng/ml human epidermal growth factor (Sigma-Aldrich), 40 ng/ml basic fibroblast growth factor (Sigma-Aldrich), 10 ng/ml fibroblast growth factor 8 (Peprotech, Rocky Hill, NJ, USA), and 10 ng/ml brain-derived neurotrophic factor (R&D Systems, Minneapolis, MN, USA). The cells were cultured in serum-free neurogenic differentiation medium for 2 weeks. At the end of the differentiation period, the cells were fixed with 4% paraformaldehyde and permeabilized with 0.5% TritonX-100/PBS. The cells were labeled with primary antibodies (1 : 200∼1 : 1,000), including rabbit anti-human glial fibrillary acidic protein (GFAP; Sigma-Aldrich), mouse anti-neuron-specific class III β-tubulin (Tuj1; Millipore, Billerica, MA, USA), and rabbit anti-microtubule- associated protein 2 (MAP2; Millipore) overnight at 4°C. After incubation with the primary antibodies, the cells were incubated for 1 h with AlexaFluor488- or AlexaFluor594-conjugated secondary antibodies (1 : 300; Molecular Probes, Carlsbad, CA, USA). The cells were subsequently stained with 4',6-diamidino-2-phenylindole (DAPI; Molecular Probes) or propidium iodide (PI; Molecular Probes) for 1 min. After mounting, the samples were analyzed by confocal microscopy (Zeiss LSM510 Meta Confocal Imaging System; Carl Zeiss, Thornwood, NY, USA). *In vitro* adipogenic, chondrogenic, hepatogenic, and osteogenic differentiation are described in the supplemental material (Supplemental Method 1).

Isolation of RNA and RT-PCR

At the end of neurogenic differentiation, total RNA was extracted using TRIzol reagent (Invitrogen, Carlsbad, CA, USA). cDNA was synthesized using the Reverse Transcription System (Promega, Madison, WI, USA). Semi-quantitative RT-PCR was performed using ExTaq DNA polymerase (Takara Biotechnology, Shiga, Japan). Amplified PCR products were electrophoresed on 1% agarose gels. PCR primer sequences are summarized in the supplemental material (Supplemental Method 2).

Microarray and genome-wide CpG methylation microarray

At the end of the neurogenic differentiation period, total RNA was isolated using TRIzol reagent. The synthesis of Target cRNA probes were synthesized and hybridized using Agilent's Low RNA Input Linear Amplification kit (Agilent Technology, Palo Alto, CA, USA) according to the manufacturer's instruction. The Cy3/5-labeled cRNA amplicon was purified on a cRNA Cleanup Module (Agilent Technology). Labeled cRNA was quantified using an ND-1000 spectrophotometer (NanoDrop Technologies, Wilmington, DE, USA). After checking the labeling efficiency, the cRNA was fragmented by adding blocking agent and fragmentation buffer and incubating at 60°C for 30 min. The cRNA fragments were resuspended in hybridization buffer and directly pipetted onto Agilent's Whole Human Genome Oligo Microarray (44K). The arrays were hybridized at 65°C for 17 h in an Agilent Hybridization oven (Agilent Technology). According to the manufacturer's protocol, the hybridized microarrays were washed. For microarray data acquisition and analysis, the hybridized arrays were scanned with Agilent's DNA microarray scanner and quantified with the Feature Extraction software (Agilent Technology). Data was normalized, and regulated genes were identified with GeneSpring GX 7.3.1 (Agilent Technology). The averages of the normalized ratios were calculated by dividing the average of the normalized signal channel intensity by the average of the normalized control channel intensity. Functional annotation of genes was carried out according to the guidelines of the Gene Ontology™ Consortium (http://www.geneontology.org/index.shtml) using GeneSpring GX 7.3.1.

For CpG methylation array analysis, genomic DNA samples from control and neurogenically differentiated hcMSCs were extracted using a Wizard Genomic DNA Purification kit (Promega). Genomic DNA was sonicated to an average fragment length of 300 bp using a VCX130 ultrasonic processor (Sonics & Materials, Newtown, CT, USA) and purified using a QIAquick PCR Purification kit (Qiagen, Valencia, CA, USA). To isolate methylated genomic DNA, 2 μg of His6-tagged methyl DNA-binding protein was incubated with 500 ng of sheared genomic DNA fragments from control and differentiated hcMSCs for 8 h at 4°C. The enriched methylated DNA was amplified using a Whole Genome Amplification kit (Sigma-Aldrich). The amplified products from control and differentiated cells were labeled with Cy3-dUTP and Cy5-dUTP, respectively, using the BioPrime Total for Agilent aCGH sys-

tem (Invitrogen). The labeled DNA samples were mixed and hybridized to a human 244K CpG island microarray (Agilent Technology). The slides were scanned with an Agilent scanner, and the images were quantified with the Feature Extraction software (Agilent Technology). Two independent experiments were performed. Data were normalized and differentially regulated genes were identified using GeneSpring GX 7.3.1 software (Agilent Technology).

RESULTS

We isolated and established several hcMSCs from a healthy donor's BM by SCM. One clone exhibited excellent multilineage plasticity. The clonal cells expressed known MSC markers, including CD29, CD44, CD73, CD90, CD105, CD133, CD166, HLA-class I, and Stro-1; however, they were negative for hematopoietic and endothelial markers, including CD14, CD31, CD34, and HLA-DR (Fig. 1A). Additionally, the cells

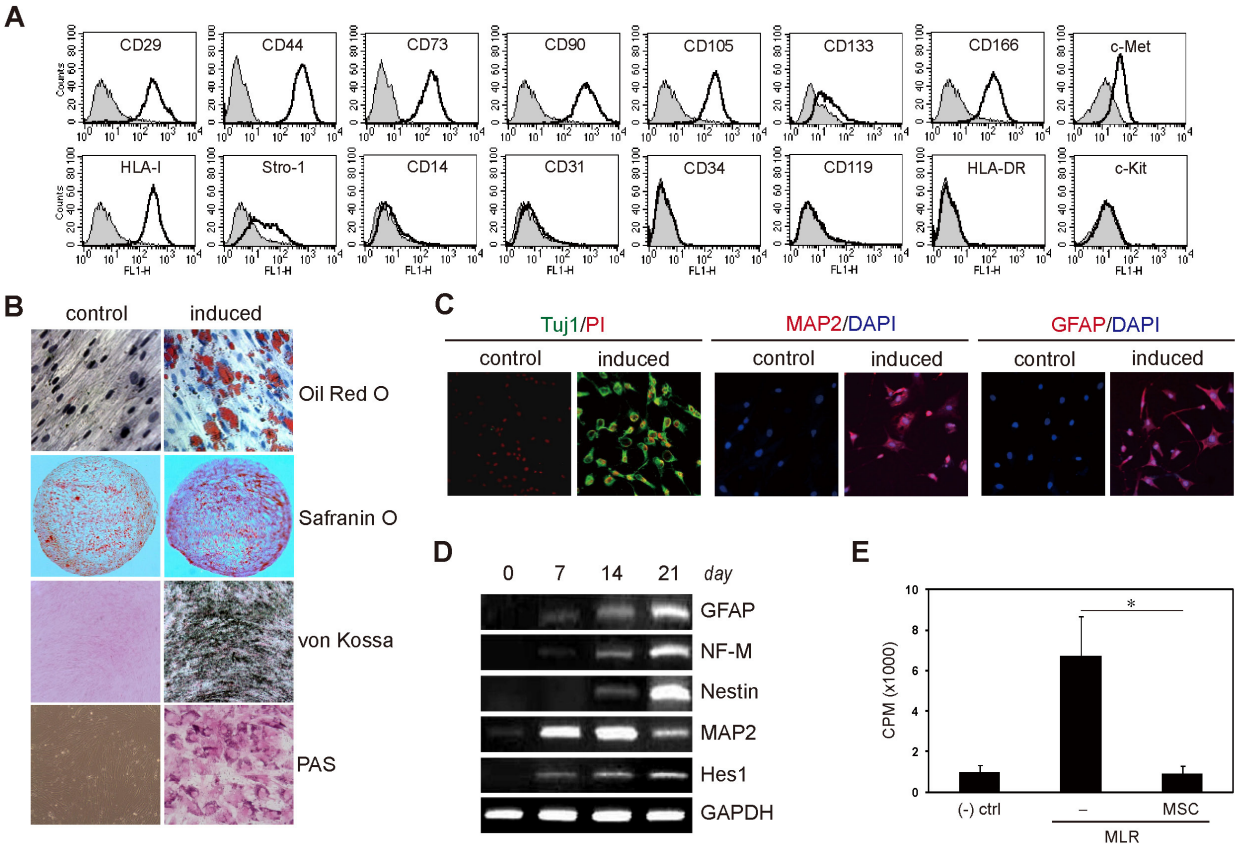

Figure 1. Characterization of hcMSCs and neural differentiation. The hcMSC line was established by SCM. (A) The cell surface markers were analyzed by flow cytometry. The cells were positive for CD29, CD44, CD73, CD90, CD105, CD133, CD166, HLA class I, Stro-1, and c-Met; however, they were negative for CD14, CD31, CD34, CD119, HLA-DR, and c-Kit. Thus, hcMSCs expressed the cell surface antigens typical of MSCs. (B) To determine the multilineage differentiation potential of the hcMSCs, the cells were cultured in adipogenic, chondrogenic, hepatogenic, and osteogenic medium to induce differentiation. Cytochemical staining showed that the cells differentiated into adipocytes (evaluated with red lipid droplets by oil red O), chondrocytes (evaluated with red glycosaminoglycans by safranin O), hepatocytes (evaluated with red glycogen deposits by periodic acid-Schiff (PAS)), and osteocytes (evaluated with black calcified nodules by von Kossa), respectively. (C) To examine the neural differentiation potential of hcMSCs, the cells were induced for 14 days, and neural marker expression was analyzed by IF staining. The differentiated cells exhibited neuronal and glial morphology and expressed several neural markers (GFAP, Tuj1, and MAP2), indicating that the hcMSC line has neural differentiation potential, as well as adipogenic, chondrogenic, hepatogenic, and osteogenic differentiation potential. (D) To confirm the neural differentiation of the hcMSCs at the molecular level, mRNA expression was analyzed. RT-PCR showed that the expression of neuronal and glial marker genes, including *NF-M, nestin, MAP2, GFAP*, and *Hes1*, increased during neural differentiation. (E) To assess the immunosuppressive activity of hcMSCs, lymphocyte proliferation in a mixed lymphocyte reaction was measured by [^{3}H]-thymidine incorporation in the presence of hcMSCs. hcMSCs significantly inhibited the proliferation of activated lymphocytes when co-cultured at a ratio of 1:5 (hcMSCs:PBMCs). (−) ctrl, negative control; *p=0.01.

were positive for c-MET, but negative for CD119 and c-Kit. The hcMSCs significantly inhibited T cell proliferation in mixed lymphocyte reactions, suggesting that they have intrinsic immunomodulatory activity (Fig. 1E). As expected, the cells successfully transdifferentiated into adipocytes, chondrocytes, hepatocytes, and osteocytes when induced *in vitro*

Table I. Top 30 upregulted or downregulated genes in neural differentaiton

No.	Upregulated genes	Gene symbol	Genbank accession no.	Fold-increase	No.	Downregulated genes	Gene symbol	Genbank accession no.	Fold-decrease
1	Proprotein convertase subtilisin/kexin type 1	PCSK1	NM_000439	42.3	1	Integrin, lpha 8	ITGA8	NM_003638	23.2
2	Matrix metallopeptidase 10 (stromelysin 2)	MMP10	NM_002425	30.1	2	Dual specificity phosphatase 18	DUSP18	NM_152511	19.4
3	Chemokine (C-X-C motif) ligand 3	CXCL3	NM_002090	24.4	3	Phosphodiesterase 11A	PDE11A	AK127194	18.7
4	Epiregulin	EREG	NM_001432	19.3	4	Phospholipase A1 member A	PLA1A	NM_015900	18.3
5	Thyrotropin-releasing hormone receptor	TRHR	NM_003301	17.7	5	Chemokine (C-C motif) ligand 2	CCL2	NM_002982	18.2
6	Tumor necrosis factor, alpha-induced protein 6	TNFAIP6	NM_007115	16.8	6	Cyclin B1	CCNB1	NM_031966	17.9
7	Interleukin 1 receptor antagonist	IL1RN	NM_173842	16.5	7	Dickkopf homolog 1	DKK1	NM_012242	17.8
8	Peroxisome proliferator-activated receptor gamma, coactivator 1 alpha	PPARGC1 A	NM_013261	14.8	8	Fibroblast growth factor 1 (acidic)	FGF1	NM_000800	13.1
9	Caudal type homeobox transcription factor 1	CDX1	NM_001804	14.2	9	Kruppel-like factor 5 (intestinal)	KLF5	NM_001730	12.4
10	Forkhead box Q1	FOXQ1	NM_033260	14.1	10	Cadherin 6, type 2, K-cadherin (fetal kidney)	CDH6	NM_004932	11.7
11	CCAAT/enhancer binding protein (C/EBP), alpha	CEBPA	NM_004364	13.1	11	Fibroblast growth factor 12	FGF12	NM_004113	11.7
12	Kynureninase (L-kynurenine hydrolase)	KYNU	D55639	10.2	12	Interleukin 13 receptor, alpha 2	IL13RA2	NM_000640	10.9
13	Neurotrophic tyrosine kinase, receptor, type 3	NTRK3	NM_001012338	10.1	13	Dystrophin (muscular dystrophy, Duchenne and Becker types)	DMD	NM_004010	10.8
14	Forkhead box F1	FOXF1	NM_001451	9.1	14	Keratin 86	KRT86	NM_002284	10.7
15	Pleckstrin homology-like domain, family A, member 1	PHLDA1	BC047362	9.0	15	Homo sapiens DNA helicase homolog (PIF1)			10.7

Table I. Continued

No.	Upregulated genes	Gene symbol	Genbank accession no.	Fold-increase	No.	Downregulated genes	Gene symbol	Genbank accession no.	Fold-decrease
16	Latent transforming growth factor beta binding protein 1	LTBP1	NM_206943	6.7	16	Sterile alpha motif domain containing 9-like	SAMD9L	NM_152703	10.7
17	Wingless-type MMTV integration site family, member 7A	WNT7A	NM_004625	5.7	17	Sortilin 1	SORT1	NM_002959	10.7
18	Prostaglandin F2 receptor negative regulator	PTGFRN	NM_020440	5.4	18	ATP-dependent RNA helicase DDX19 (DEAD-box protein 19)			10.6
19	SRY (sex determining region Y)-box 4	SOX4	NM_003107	5.4	19	Chromosome 20 open reading frame 197	C20orf197	NM_173644	10.6
20	Matrix metallopeptidase 14 (membrane-inserted)	MMP14	NM_004995	5.4	20	Interferon-induced protein with tetratricopeptide repeats 1	IFIT1	NM_001548	10.6
21	Stanniocalcin 1	STC1	NM_003155	5.1	21	Interferon, alpha-inducible protein 27	IFI27	NM_005532	10.6
22	Protein kinase, cAMP-dependent, regulatory, type I, alpha (tissue specific extinguisher 1)	PRKAR1A	NM_212472	5.1	22	Connective tissue growth factor	CTGF	NM_001901	10.6
23	Vascular endothelial growth factor A	VEGFA	NM_001025366	5.0	23	Integrin, alpha 6	ITGA6	NM_000210	9.5
24	Homeobox A6	HOXA6	NM_024014	4.9	24	CD36 molecule (thrombospondin receptor)	CD36	AW450111	9.2
25	Synaptotagmin III	SYT3	NM_032298	4.9	25	Poly (ADP-ribose) polymerase family, member 14	PARP14	NM_017554	8.0
26	Tumor necrosis factor receptor superfamily, member 1A	TNFRSF1A	NM_001065	4.7	26	Cadherin 1, type 1, E-cadherin (epithelial)	CDH1	NM_004360	7.8
27	Hepatocyte growth factor (hepapoietin A; scatter factor)	HGF	NM_001010931	4.5	27	CAP, adenylate cyclase-associated protein, 2 (yeast)	CAP2	NM_006366	7.7
28	Tumor necrosis factor receptor superfamily, member 19	TNFRSF19	NM_148957	4.5	28	Neural precursor cell expressed, developmentally down-regulated 9	NEDD9	NM_006403	7.7
29	EPH receptor A4	EPHA4	NM_004438	4.4	29	Proprotein convertase subtilisin/kexin type 7	PCSK7	NM_004716	7.7
30	Musashi homolog 1 (Drosophila)	MSI1	NM_002442	4.4	30	Mitogen activated protein kinase binding protein 1	MAPKBP1	NM_014994	7.4

with adipogenic, chondrogenic, hepatogenic, and osteogenic medium, respectively (Fig. 1B). Additionally, the cells exhibited a neural phenotype when cultured in the appropriate induction medium. After 14 days of differentiation, the cells were fixed and stained for IF analysis. When examined by confocal microscopy, the induced cells were positive for the neuronal and glial markers Tuj1, MAP2, and GFAP (Fig. 1C). GFAP, neurofilament M (NFM), nestin, MAP2, and Hes1 mRNA levels increased during neural differentiation (Fig. 1D). The mRNA levels of these neuroglial maker genes were increased or maintained for up to 21 days. These results showed that the hcMSC line could acquire a neural phenotype after appropriate induction.

Although neuronal expression profiles of BM-derived MSCs have been reported (22,24), to our knowledge, no study has assessed a homogeneous MSC population. We chose homogeneous hcMSCs rather than heterogeneous MSC pools in order to improve the reliability of the gene expression data and to eliminate the mixed information obtained from a heterogeneous MSC population. Two independent RNA samples from the hcMSC line were isolated before and after neural induction for 14 days and then subjected to microarray analysis. The average value of the two independent results was used for data analysis.

The microarray probe set included 27,958 genes. A 2-fold increase over expression in control cells was selected as the threshold for upregulated genes, and a 2-fold decrease was selected as the threshold for downregulated genes. With these criteria, we identified 1025 upregulated genes and 1415 downregulated genes. Table I shows the top 30 upregulated genes and the top 30 downregulated genes in differentiated MSCs. During neural differentiation, the expression of *PCSK1, MMP10*, and *CXCL3* increased 42.3-fold, 30.1-fold, and 24.4-fold, respectively. Conversely, *ITGA8, DUSP18*, and *DKK1* decreased 23.2-fold, 19.4-fold, and 17.8-fold, respectively. The genes were sorted and classified into several groups according to gene ontology. We examined the data with respect to neuronal differentiation or nervous system differentiation (Supplemental Table). Forty-three genes, including *Ereg*, neurotrophic tyrosine kinase receptor 3 (*NTrk3*), Musashi homolog 1 (*MSI1*), *Sema4G, NDRG2, Amigo1, EphrinB1, Notch3,* and *Pax6* were upregulated, whereas only 3 genes (*MyD88, GDAP2*, and *RQCD1*) were downregulated. *NTrk3, Notch3, NDRG2, MSI1, Amigo1, Sema4G*, and *EphrinB1* play important roles in neurogenesis. The fact that these upregulated genes are involved in neuronal differentiation and nervous system development provides evidence of the genuine neurogenic potential of MSCs, refuting some controversial studies that suggest a false-positive gain of neural phenotype in MSCs treated with neural induction reagents.

To verify the gene expression profile generated by the microarray analysis, genes were randomly selected for evaluation by RT-PCR (Fig. 2). The expression of *PCSK, Ereg, MMP10, Cdx1, Wnt7a, Sox4,* and *MEPE* increased, whereas the expression of *Smad3, Smurf2, NEDD4L, STAT1, DAAM2, ITGA6*, and *DKK1* decreased. These results were consistent with the microarray data, indicating that our microarray experiments were highly reliable.

To generate additional gene expression data, we examined epigenetic changes by analyzing promoter methylation and compared the results with the gene expression profile. DNA methylation is a key epigenetic regulatory mechanism for development and gene expression (25,26) that typically occurs at CpG dinucleotides. Clusters of CpG dinucleotides, called CpG islands, are usually found in mammalian gene promoters

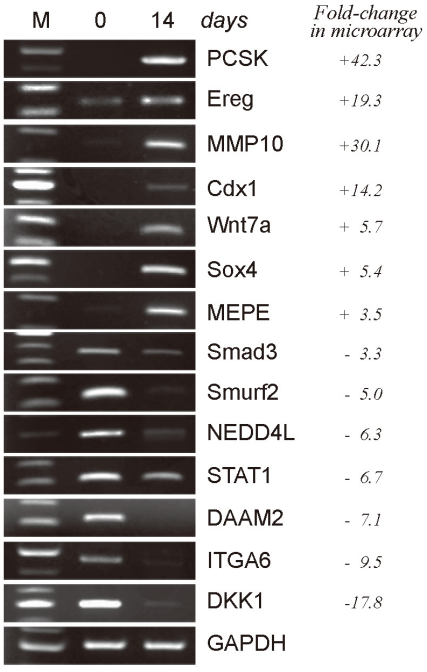

Figure 2. RT-PCR confirmation of the gene expression changes observed in the microarray analysis of neurally differentiated hcMSCs. After the hcMSCs were differentiated for 14 days, mRNA was extracted and subjected to microarray analysis. To confirm the microarray data, the expression of randomly selected genes that changed 2-fold or more in the microarray analysis was assessed by RT-PCR. + denotes increase and − represents decrease.

(27). Methylation of the CpG islands in a promoter region inhibits gene expression, whereas lack of methylation permits gene expression (28). Therefore, examining the CpG methylation status of promoters may provide further insight into gene expression during the neural differentiation of MSCs. We isolated genomic DNA from hcMSCs before and after neu-

Table II. Promoter methylation patterns of some differentially expressed genes

No.	Upregulated & hypomethylated genes	Gene symbol	GenBank accession no.
1	Neurotrophic tyrosine kinase, receptor, type 3	NTRK3	NM_001012338
2	ST8 alpha-N-acetyl-neuraminide alpha-2,8-sialyltransferase 5	ST8SIA5	NM_013305
3	Prostaglandin F2 receptor negative regulator	PTGFRN	NM_020440
4	SRY (sex determining region Y)-box 4	SOX4	NM_003107
5	Synaptotagmin III	SYT3	NM_032298
6	Chromatin modifying protein 1B	CHMP1B	NM_020412
7	Fatty acid binding protein 5 (psoriasis-associated)	FABP5	NM_001444
8	Collagen, type XVIII, alpha 1	COL18A1	NM_030582
9	Calcium modulating ligand	CAMLG	NM_001745
10	CUB domain containing protein 1	CDCP1	NM_178181
11	Glutamate receptor, ionotrophic, AMPA 4	GRIA4	NM_000829
12	Zinc finger protein 331	ZNF331	NM_018555
13	Neurexophilin 4	NXPH4	NM_007224
14	Forkhead box C1	FOXC1	NM_001453
15	Protein kinase, membrane associated tyrosine/threonine 1	PKMYT1	NM_004203
16	Chromosome 3 open reading frame 58	C3orf58	NM_173552
17	BarH-like 2 (Drosophila)	BARHL2	NM_020063
18	Papilin, proteoglycan-like sulfated glycoprotein	PAPLN	NM_173462
19	Paired box gene 6 (aniridia, keratitis)	PAX6	NM_001604
20	Treacher Collins-Franceschetti syndrome 1	TCOF1	NM_001008656
No.	Downregulated & hypermethylated genes	Gene symbol	GenBank accession no.
1	Neurexin 3	NRXN3	NM_004796
2	Ribonucleotide reductase M2 polypeptide	RRM2	NM_001034
3	Kelch domain containing 4	KLHDC4	NM_017566
4	Homer homolog 2 (Drosophila)	HOMER2	NM_199330
5	Natriuretic peptide receptor C/guanylate cyclase C	NPR3	NM_000908
6	CDC42 effector protein (Rho GTPase binding) 3	CDC42EP3	NM_006449
7	Neural precursor cell expressed, developmentally down-regulated 4-like	NEDD4L	NM_015277
8	Adenylate kinase 5	AK5	NM_174858
9	WD repeat domain 1	WDR1	NM_017491
10	v-yes-1 Yamaguchi sarcoma viral related oncogene homolog	LYN	NM_002350
11	Aryl-hydrocarbon receptor nuclear translocator 2	ARNT2	NM_014862
12	Solute carrier family 38, member 2	SLC38A2	NM_018976
13	RAB35, member RAS oncogene family	RAB35	NM_006861
14	Chromosome 14 open reading frame 106	C14orf106	NM_018353
15	Ras and Rab interactor 3	RIN3	NM_024832
16	Protein arginine methyltransferase 2	PRMT2	NM_206962
17	WD repeat domain 1	WDR1	NM_017491
18	Signal-regulatory protein alpha	SIRPA	NM_080792
19	Palladin, cytoskeletal associated protein	PALLD	NM_016081
20	DEK oncogene (DNA binding)	DEK	NM_003472

ral induction for 14 days and used CpG methylation microarray analysis to determine the genome-wide methylation profile.

In differentiated hcMSCs, 1141 promoters were hypermethylated (≥2-fold increase) and 1276 promoters were hypomethylated (≥2-fold decrease) when compared with promoters in control hcMSCs. Among the hypomethylated genes, we looked for genes that were upregulated ≥2-fold in the microarray data. Similarly, among the hypermethylated genes, we looked for genes that were downregulated ≥2-fold in the microarray data. We identified 50 genes whose expression was upregulated and whose promoters were hypomethylated, along with 68 genes with downregulated expression and hypermethylated promoters (Table II). The genes that were upregulated and hypomethylated included *NTrk3, Sox4, SYTIII, FABP5, GRIA4, NXPH4, FoxC1, BARHL2, PAPLN*, and *Pax6*. Among these genes, *NTrk3* and *Sox4* belonged to the group of 30 genes with the highest expression in differentiated hcMSCs, as listed in Table I. Most of genes in Table II are involved in neurogenesis or nervous system development, confirming the high fidelity of our microarray data. Genes that were downregulated and hypermethylated included *NRXN3, Cdc42EP3, NEDD4L, SIRP*α, and *DEK*.

DISCUSSION

Microarray technology enables easy comparison of the differential expression of a large number of genes. However, false-positive results present an obstacle to microarray data analysis. Given that microarray experiments are likely to show variation in their results, sample quality is another critical factor in the analysis. Some studies have determined the gene expression profiles of neural differentiation in MSCs using microarray analysis (16,24). The most common method for isolating MSCs is Ficoll-mediated density gradient centrifugation. The resulting MSC pool is heterogeneous because no additional purification process is used in this method. Even the defined sorting method, which uses specific antibodies, might not completely eliminate heterogeneity in the isolated MSC population. We previously developed an easy and simple isolation method for obtaining hcMSCs called SCM (21). Because no reports have described microarray analysis of a homogeneous MSC population, we examined the gene expression profile of neurally differentiated hcMSCs. The microarray results were confirmed with RT-PCR analysis. In addition, we combined the microarray data with independent promoter methylation chip array data to generate more accurate information.

According to the gene ontology analysis, the expression of neuronal-specific genes involved in neuronal differentiation and nervous system differentiation increased in neurally differentiated hcMSCs (Supplemental Table). Genes involved in synaptic transmission, such as *EGR3* (listed in Supplemental Table), *SYT3* (listed in Table II), nicotinic cholinergic receptor 5 (not listed, 4.5-fold increase), glycine receptor alpha 3 (not listed, 4.4-fold increase), protocadherin beta 13 (not listed, 3.1-fold increase), neurotensin receptor 1 (not listed, 2.1-fold increase), and a voltage-dependent calcium channel (not listed, 2.1-fold increase), were upregulated. Genes encoding channel proteins, including a voltage-gated potassium channel, a glycine receptor, glutamate receptors, nicotinic cholinergic receptors, and a voltage-dependent calcium channel, were also upregulated (not listed).

The canonical Wnt signaling pathway plays an important role in neurogenesis (29,30). According to our microarray analysis, the Wnt signaling molecule Wnt7a was highly upregulated at the mRNA level, whereas DKK1, a Wnt signaling inhibitor, was significantly downregulated 17.8-fold (Table I). This is consistent with reports describing the functional role of Wnt signaling in neurogenesis (31,32). With regard to Wnt signaling molecules, the genes encoding Axin2 and FZD10 were upregulated, and those encoding TLE4 and DACT1 were downregulated in our microarray analysis (not listed). These results are consistent with those of a recent study demonstrating that FZD10 promotes the development of sensory neurons (33).

One of the interesting gene groups identified in this study comprised E3 ubiquitin protein ligases, which catalyze protein ubiquitination (34,35). Protein ubiquitination is catalyzed by three groups of enzymes, ubiquitin-activating E1 enzymes, ubiquitin-conjugating E2 enzymes, and ubiquitin-ligating E3 ligases. Functionally, the E3 ligase determines which proteins are ubiquitinated. There are two types of E3 ligases: the RING type and the HECT type (36,37). In humans, most E3 ligases are RING-type enzymes; only 28 ligases are HECT-type enzymes, such as those in the HERC family and NEDD4 family (36,37). In neurally differentiated hcMSCs, the gene encoding NEDD4L was downregulated and its promoter was hypermethylated (Table II). Other E3 ubiquitin protein ligase genes, including *Smurf2* (not listed, 4.2-fold decrease), *WWP2* (not listed, 2.3-fold decrease), and *NEDD4* (not listed, 6.4-fold decrease), were also downregulated when assessed by micro-

array analysis. Notably, these genes belong to the NEDD4 family of HECT-type E3 ligases (37). Ubiquitination of Rap1B by Smurf2 is required for neuronal polarity (38). Downregulation of *Smurf2* expression was confirmed by RT-PCR analysis (Fig. 2). Smurf1 regulates neurite extension through Rho GTPase (39). On the other hand, the expression of other E3 ligase genes increased, including *TRIM50* and *RNF25* (data not shown). Interestingly, TRIM50 and RNF25 are members of the RING-type E3 ligase family. Future studies will determine whether downregulation of specific HECT-type E3 ubiquitin ligases, such as NEDD4L and Smurf2, is functionally correlated with the acquired neuronal phenotype of MSCs. Smurf2 might be a good candidate for future study because its downregulated expression was verified by RT-PCR (Fig. 2).

Finally, it is notable that *TNFAIP6* (16.8-fold increase) and *IL1RN* (16.5-fold increase) were highly upregulated in neurally differentiated hcMSCs (Table I). TNFAIP6, also called TSG-6, plays a critical role in MSC-mediated immunosuppression (40). TNFAIP6 reduces various inflammatory conditions, including myocardial infarction, zymosan-induced peritonitis, and corneal injury (41-43). *IL1RN* encodes interleukin-1 receptor antagonist (IL-1Ra), which can modulate various IL-1-related inflammatory responses by inhibiting IL-1 α and IL-1 β (44). Anakinra, an approved IL-1Ra drug used to treat rheumatoid arthritis, has therapeutic effects on a variety of local, systemic, hereditary autoimmune inflammatory diseases (45).

We evaluated the gene expression profile of neurally differentiated MSCs using homogeneous clonal cells. To verify the gene expression profile, we confirmed the results from the microarray analysis with RT-PCR and analyzed data obtained from CpG methylation microarray analysis. Our results provide evidence for the neuronal and glial potency of MSCs. Thus, MSCs can be used for the development of cell therapies that target neuroimmune disorders such as stroke, multiple sclerosis, and Parkinson's disease. The upregulation of some anti-inflammatory genes, such as *TNFAIP6* and *IL1RN*, during neural differentiation improves the outlook on the therapeutic utility of MSCs. Furthermore, neurogenically induced or neurogenically primed hcMSCs retained their immunosuppressive activity against activated T cells *in vitro* (unpublished data). Thus, an optimized balance between the immunomodulatory activity and neurogenic potency of MSCs may provide a new therapeutic solution for incurable neuroimmune diseases. Although our study is only one small step toward understanding the biological and molecular properties of MSCs, further investigation should contribute to the development of stem cell therapy.

ACKNOWLEDGEMENTS

This study was supported by the Bio & Medical Technology Development Program (NRF-2011-0019634 and NRF-2011-0019637) of the National Research Foundation of the Korean government (MEST), and by a grant from Inha University (44773-01).

CONFLICTS OF INTEREST

The authors have no financial conflict of interest.

REFERENCES

1. Friedenstein, A. J., K. V. Petrakova, A. I. Kurolesova, and G. P. Frolova. 1968. Heterotopic of bone marrow; Analysis of precursor cells for osteogenic and hematopoietic tissues. *Transplantation* 6: 230-247.
2. Bernardo, M. E., F. Locatelli, and W. E. Fibbe. 2009. Mesenchymal stromal cells. *Ann. N. Y. Acad. Sci.* 1176: 101-117.
3. Yi, T. and S. U. Song. 2012. Immunomodulatory properties of mesenchymal stem cells and their therapeutic applications. *Arch. Pharm. Res.* 35: 213-221.
4. Yoo, H. S., T. Yi, Y. K. Cho, W. C. Kim, S. U. Song, and M. S. Jeon. 2013. Mesenchymal stem cell lines isolated by different isolation methods show variations in the regulation of graft-versus-host disease. *Immune Netw.* 13: 133-140.
5. Anderson, P., L. Souza-Moreira, M. Morell, M. Caro, F. O'Valle, E. Gonzalez-Rey, and M. Delgado. 2013. Adipose-derived mesenchymal stromal cells induce immunomodulatory macrophages which protect from experimental colitis and sepsis. *Gut* 62: 1131-1141.
6. Jung, K. H., S. U. Song, T. Yi, M. S. Jeon, S. W. Hong, H. M. Zheng, H. S. Lee, M. J. Choi, D. H. Lee, and S. S. Hong. 2011. Human bone marrow-derived clonal mesenchymal stem cells inhibit inflammation and reduce acute pancreatitis in rats. *Gastroenterology* 140: 998-1008.
7. Pittenger, M. F., A. M. Mackay, S. C. Beck, R. K. Jaiswal, R. Douglas, J. D. Mosca, M. A. Moorman, D. W. Simonetti, S. Craig, and D. R. Marshak. 1999. Multilineage potential of adult human mesenchymal stem cells. *Science* 284: 143-147.
8. Wang, G., B. A. Bunnell, R. G. Painter, B. C. Quiniones, S. Tom, N. A. Lanson, Jr., J. L. Spees, D. Bertucci, A. Peister, D. J. Weiss, V. G. Valentine, D. J. Prockop, and J. K. Kolls. 2005. Adult stem cells from bone marrow stroma differentiate into airway epithelial cells: potential therapy for cystic fibrosis. *Proc. Natl. Acad. Sci. USA* 102: 186-191.
9. Tao, X. R., W. L. Li, J. Su, C. X. Jin, X. M. Wang, J. X.

Li, J. K. Hu, Z. H. Xiang, J. T. Lau, and Y. P. Hu. 2009. Clonal mesenchymal stem cells derived from human bone marrow can differentiate into hepatocyte-like cells in injured livers of SCID mice. *J. Cell. Biochem.* 108: 693-704.
10. Hofstetter, C. P., E. J. Schwarz, D. Hess, J. Widenfalk, A. El Manira, D. J. Prockop, and L. Olson. 2002. Marrow stromal cells form guiding strands in the injured spinal cord and promote recovery. *Proc. Natl. Acad. Sci. USA* 99: 2199-2204.
11. Woodbury, D., E. J. Schwarz, D. J. Prockop, and I. B. Black. 2000. Adult rat and human bone marrow stromal cells differentiate into neurons. *J. Neurosci. Res.* 61: 364-370.
12. Deng, W., M. Obrocka, I. Fischer, and D. J. Prockop. 2001. *In vitro* differentiation of human marrow stromal cells into early progenitors of neural cells by conditions that increase intracellular cyclic AMP. *Biochem. Biophys. Res. Commun.* 282: 148-152.
13. Neuhuber, B., G. Gallo, L. Howard, L. Kostura, A. Mackay, and I. Fischer. 2004. Reevaluation of *in vitro* differentiation protocols for bone marrow stromal cells: disruption of actin cytoskeleton induces rapid morphological changes and mimics neuronal phenotype. *J. Neurosci. Res.* 77: 192-204.
14. Lu, P., A. Blesch, and M. H. Tuszynski. 2004. Induction of bone marrow stromal cells to neurons: differentiation, transdifferentiation, or artifact? *J. Neurosci. Res.* 77: 174-191.
15. Mareschi, K., M. Novara, D. Rustichelli, I. Ferrero, D. Guido, E. Carbone, E. Medico, E. Madon, A. Vercelli, and F. Fagioli. 2006. Neural differentiation of human mesenchymal stem cells: Evidence for expression of neural markers and eag K+ channel types. *Exp. Hematol.* 34: 1563-1572.
16. Kim, S., O. Honmou, K. Kato, T. Nonaka, K. Houkin, H. Hamada, and J. D. Kocsis. 2006. Neural differentiation potential of peripheral blood- and bone-marrow-derived precursor cells. *Brain Res.* 1123: 27-33.
17. Ankrum, J. and J. M. Karp. 2010. Mesenchymal stem cell therapy: two steps forward, one step back. *Trends Mol. Med.* 16: 203-209.
18. Einstein, O., N. Fainstein, I. Vaknin, R. Mizrachi-Kol, E. Reihartz, N. Grigoriadis, I. Lavon, M. Baniyash, H. Lassmann, and T. Ben-Hur. 2007. Neural precursors attenuate autoimmune encephalomyelitis by peripheral immunosuppression. *Ann. Neurol.* 61: 209-218.
19. Ben-Hur, T. 2008. Immunomodulation by neural stem cells. *J. Neurol. Sci.* 265: 102-104.
20. Rickard, D. J., M. Kassem, T. E. Hefferan, G. Sarkar, T. C. Spelsberg, and B. L. Riggs. 1996. Isolation and characterization of osteoblast precursor cells from human bone marrow. *J. Bone Miner. Res.* 11: 312-324.
21. Song, S. U., C. S. Kim, S. P. Yoon, S. K. Kim, M. H. Lee, J. S. Kang, G. S. Choi, S. H. Moon, M. S. Choi, Y. K. Cho, and B. K. Son. 2008. Variations of clonal marrow stem cell lines established from human bone marrow in surface epitopes, differentiation potential, gene expression, and cytokine secretion. *Stem Cells Dev.* 17: 451-461.
22. Tondreau, T., M. Dejeneffe, N. Meuleman, B. Stamatopoulos, A. Delforge, P. Martiat, D. Bron, and L. Lagneaux. 2008. Gene expression pattern of functional neuronal cells derived from human bone marrow mesenchymal stromal cells. *BMC Genomics* 9: 166-176.
23. Shakhbazov, A. V., N. V. Goncharova, S. M. Kosmacheva, N. A. Kartel, and M. P. Potanev. 2009. Plasticity of human msesnchymal stem cell phenotype and expression profile under neurogenic conditions. *Cell Technol. Biol. Med.* 2: 513-516.
24. Yamaguchi, S., S. Kuroda, H. Kobayashi, H. Shichinohe, S. Yano, K. Hida, K. Shinpo, S. Kikuchi, and Y. Iwasaki. 2006. The effects of neuronal induction on gene expression profile in bone marrow stromal cells (BMSC)-a preliminary study using microarray analysis. *Brain Res.* 1087: 15-27.
25. Reik, W., W. Dean, and J. Walter. 2001. Epigenetic reprogramming in mammalian development. *Science* 293: 1089-1093.
26. Jaenisch, R. and A. Bird. 2003. Epigenetic regulation of gene expression: how the genome integrates intrinsic and environmental signals. *Nat. Genet.* 33 Suppl: 245-254.
27. Larsen, F., G. Gundersen, R. Lopez, and H. Prydz. 1992. CpG islands as gene markers in the human genome. *Genomics* 13: 1095-1107.
28. Bird, A. P. and A. P. Wolffe. 1999. Methylation-induced repression--belts, braces, and chromatin. *Cell* 99: 451-454.
29. Lee, J. E., S. F. Wu, L. M. Goering, and R. I. Dorsky. 2006. Canonical Wnt signaling through Lef1 is required for hypothalamic neurogenesis. *Development* 133: 4451-4461.
30. Gulacsi, A. A. and S. A. Anderson. 2008. Beta-catenin-mediated Wnt signaling regulates neurogenesis in the ventral telencephalon. *Nat. Neurosci.* 11: 1383-1391.
31. Toledo, E. M., M. Colombres, and N. C. Inestrosa. 2008. Wnt signaling in neuroprotection and stem cell differentiation. *Prog. Neurobiol.* 86: 281-296.
32. Kuwabara, T., J. Hsieh, A. Muotri, G. Yeo, M. Warashina, D. C. Lie, L. Moore, K. Nakashima, M. Asashima, and F. H. Gage. 2009. Wnt-mediated activation of NeuroD1 and retroelements during adult neurogenesis. *Nat. Neurosci.* 12: 1097-1105.
33. Garcia-Morales, C., C. H. Liu, M. Abu-Elmagd, M. K. Hajihosseini, and G. N. Wheeler. 2009. Frizzled-10 promotes sensory neuron development in Xenopus embryos. *Dev. Biol.* 335: 143-155.
34. Ardley, H. C. and P. A. Robinson. 2005. E3 ubiquitin ligases, *Essays Biochem.* 41: 15-30.
35. Deshaies, R. J. and C. A. Joazeiro. 2009. RING domain E3 ubiquitin ligases. *Annu. Rev. Biochem.* 78: 399-434.
36. Li, W., M. H. Bengtson, A. Ulbrich, A. Matsuda, V. A. Reddy, A. Orth, S. K. Chanda, S. Batalov, and C. A. Joazeiro. 2008. Genome-wide and functional annotation of human E3 ubiquitin ligases identifies MULAN, a mitochondrial E3 that regulates the organelle's dynamics and signaling. *PLoS One* 3: e1487.
37. Rotin, D. and S. Kumar. 2009. Physiological functions of the HECT family of ubiquitin ligases. *Nat. Rev. Mol. Cell Biol.* 10: 398-409.
38. Schwamborn, J. C., M. Muller, A. H. Becker, and A. W. Puschel. 2007. Ubiquitination of the GTPase Rap1B by the ubiquitin ligase Smurf2 is required for the establishment of neuronal polarity. *EMBO J.* 26: 1410-1422.
39. Bryan, B., Y. Cai, K. Wrighton, G. Wu, X. H. Feng, and M. Liu. 2005. Ubiquitination of RhoA by Smurf1 promotes neu-

rite outgrowth. *FEBS Lett.* 579: 1015-1019.
40. Prockop, D. J. and J. Y. Oh. 2012. Mesenchymal stem/stromal cells (MSCs): role as guardians of inflammation. *Mol. Ther.* 20: 14-20.
41. Lee, R. H., A. A. Pulin, M. J. Seo, D. J. Kota, J. Ylostalo, B. L. Larson, L. Semprun-Prieto, P. Delafontaine, and D. J. Prockop. 2009. Intravenous hMSCs improve myocardial infarction in mice because cells embolized in lung are activated to secrete the anti-inflammatory protein TSG-6. *Cell Stem Cell* 5: 54-63.
42. Oh, J. Y., G. W. Roddy, H. Choi, R. H. Lee, J. H. Ylostalo, R. H. Rosa, Jr., and D. J. Prockop. 2010. Antiinflammatory protein TSG-6 reduces inflammatory damage to the cornea following chemical and mechanical injury. *Proc. Natl. Acad. Sci. USA* 107: 16875-16880.
43. Choi, H., R. H. Lee, N. Bazhanov, J. Y. Oh, and D. J. Prockop. 2011. Anti-inflammatory protein TSG-6 secreted by activated MSCs attenuates zymosan-induced mouse peritonitis by decreasing TLR2/NF-κB signaling in resident macrophages. *Blood* 118: 330-338.
44. Dripps, D. J., B. J. Brandhuber, R. C. Thompson, and S. P. Eisenberg. 1991. Interleukin-1 (IL-1) receptor antagonist binds to the 80-kDa IL-1 receptor but does not initiate IL-1 signal transduction. *J. Biol. Chem.* 266: 10331-10336.
45. Dinarello, C. A., A. Simon, and J. W. van der Meer. 2012. Treating inflammation by blocking interleukin-1 in a broad spectrum of diseases. *Nat. Rev. Drug Discov.* 11: 633-652.